Proceedings of the 2nd International Congress APMAS2012, April 26–29, 2012, Antalya, Turkey

Enhancement of Electron Mobility and Photoconductivity in Quantum Well $In_{0.52}Al_{0.48}As/In_{0.53}Ga_{0.47}As/In_{0.52}Al_{0.48}As$ on InP Substrate

V.A. Kulbachinskii*, R.A. Lunin, N.A. Yuzeeva, G.B. Galiev, I.S. Vasilievskii and E.A. Klimov

Moscow State University (M.V. Lomonosov), Physics Faculty, Low Temperature Physics and Superconductivity Department, Moscow, 119991 GSP-1, Russia

Isomorphic $In_{0.52}Al_{0.48}As/In_{0.53}Ga_{0.47}As/In_{0.52}Al_{0.48}As$ quantum well structure on InP substrate were grown by molecular beam epitaxy. We investigated the electron transport properties and mobility enhancement in the structures by changing of doping level, the width d of quantum well $In_{0.53}Ga_{0.47}As$ or by illumination using light with $\lambda = 668$ nm. Persistent photoconductivity was observed in all samples due to spatial separation of carriers. We used the Shubnikov–de Haas effect to analyze subband electron concentration and mobility. The maximal mobility was observed for quantum well width $d = 16$ nm.

DOI: 10.12693/APhysPolA.123.345

PACS: 72.10.−d, 73.21.Fg, 73.63.Hs

1. Introduction

There is a significant interest to InAlAs/InGaAs heterostructures on InP substrate. One of the reasons is the advantage of such structures. They allowed using the wider frequency range and having lower electronic noise. The possibility to increase the InAs content in the InGaAs layer up to 70% and higher gives an opportunity to increase mobility, electron concentration in the channel and the drift velocity of electrons. Isomorphic or pseudomorphic InGaAs structures on InP substrate may be used for different applications. In one of the first Ref. [1] matched heterostructures InAlAs/InGaAs/InAlAs on InP substrate were grown. The electron mobility and concentration were investigated as a function of the width of spacer and quantum well InGaAs width d. Later for high electron mobility transisitor (HEMT) isomorphic heterostructures on InP substrate with channel $d = 20$ nm and spacer 2 nm were used [2]. It is known also that inserted InAs layers and composite conducting channel with shortness of the gate improved the UHF characteristics of transistors [3].

In this research we investigated the electron transport properties and mobility enhancement in the ternary structures $In_{0.52}Al_{0.48}As/In_{0.53}Ga_{0.47}As/In_{0.52}Al_{0.48}As$ on InP substrate by changing of doping level, the width d of isomorphic quantum well $In_{0.53}Ga_{0.47}As$ or by illumination using light with $\lambda = 668$ nm. We used the Shubnikov–de Haas (SdH) effect to analyze subband electron concentration and mobility and their dependence on doping level, quantum well width and illumination.

2. Experimental

The samples were grown by the molecular beam epitaxy on InP (100) substrates. All samples have $In_{0.52}Al_{0.48}As$ buffer matched (isomorphic) to InP. Samples have one-side delta-doping by Si. The spacer thickness was 4.3–6.0 nm. Cap layer was undoped $In_{0.53}Ga_{0.47}As$.

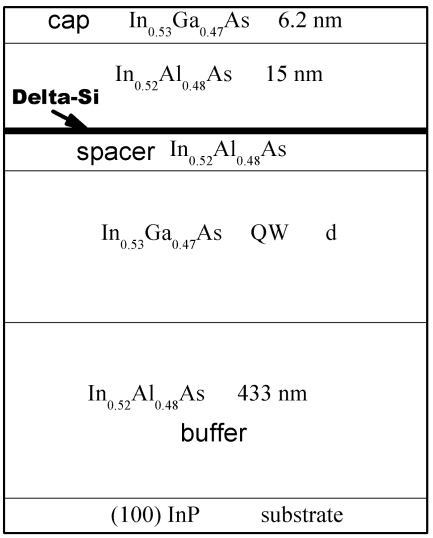

Fig. 1. Schematic diagram of the $In_{0.52}Al_{0.48}As/In_{0.53}Ga_{0.47}As/In_{0.52}Al_{0.48}As$ structure on InP substrate.

Schematic diagram of the $In_{0.52}Al_{0.48}As/In_xGa_{1-x}As/In_{0.52}Al_{0.48}As$ structure on InP substrate is shown in Fig. 1. Temperature dependence of the resistance and the Hall effect were measured in the temperature interval 4.2 K $< T <$ 300 K. At $T = 4.2$ K SdH effect was investigated in magnetic field provided by a superconducting solenoid up to 6 T. We found that mobility depends on doping and width of quantum well. Some experimental parameters of samples at $T = 4.2$ K are listed in Table I.

*corresponding author; e-mail: kulb@mig.phys.msu.ru

TABLE I

Some parameters of samples: quantum well width d, Hall concentration n_H and mobility μ_H at 4.2 K, electron concentration determined from SdH effect in 1st n_1 and 2nd n_2 subbands.

Sample #	d [nm]	n_H [10^{12} cm^{-2}] (dark)	μ_H [cm^2/(V s)] (dark)	μ_H [cm^2/(V s)] (illuminated)	n_1 (n_2) [10^{12} cm^{-2}] (dark)	n_1 (n_2) [10^{12} cm^{-2}] (illuminated)
1	26	3.2	40 000	41 000	2.49 (0.70)	2.50 (0.74)
2	18.5	2.6	45 800	46 900	2.00 (0.59)	2.20 (0.7)
3	16	1.95	53 500	60 000	1.67 (0.26)	1.87 (0.53)
4	14.5	1.6	45 000	52 400	1.55 (-)	2.08 (-)

TABLE III

Quantum μ_q and transport μ_t mobilities, subband electron concentrations at $T = 4.2$ K.

Sample 3	Subband #	n_{SdH} [10^{12} cm^{-2}] experiment	μ_q [cm^2/(V s)]	μ_t [cm^2/(V s)]
dark	2	0.26	3900	72000
	1	1.67	2100	86900
illuminated	2	0.53	6700	183000
	1	1.87	2700	138000

3. Results and discussion

We observed two frequencies corresponding to two filled subbands in SdH effect in all samples except sample #4 due to much less doping of this sample. We use conventional fast Fourier transform (FFT) of the SdH oscillations to obtain the electron subband concentrations n_i from the frequencies of oscillations. Under illumination subband electron concentrations and the Hall mobilities μ_H increased (see Table I). When a sufficiently high electron concentration is produced by doping (sample 1) the illumination changed the electron concentration much less with respect to the less doped samples. In Fig. 2a SdH oscillation is shown for sample 2 in dark (solid line) and under illumination (dashed line). Fast Fourier transform spectra are shown in Fig. 2b.

Persistent photoconductivity was observed in all samples. The typical dependences of the resistance on temperature and illumination are shown in Fig. 3a for two different samples. The samples were illuminated at $T =$ 4.2 K to achieve the saturation of its resistance, then the illumination was switched off and the temperature dependence of the resistance was measured with the rate 5 K/min. At $T >$ 160–170 K, the difference between resistances measured in the dark and after illumination became less than the error of measurements.

The effect of persistent photoconductivity is related to the spatial separation of carriers. This fact is confirmed by the logarithmic dependence of the photoconductivity relaxation on time in the initial time interval $\Delta\sigma = \sigma(0) - \sigma(t) = A\ln(1 + t/\tau)$ [4, 5] with the value of τ in the range 20–30 s. Relaxation and fitting of conductivity for sample 2 is shown in Fig. 3b.

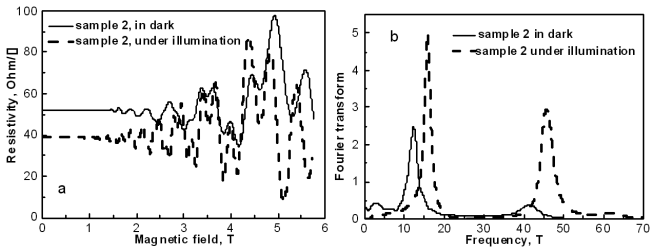

Fig. 2. (a) Magnetoresistance oscillation in sample 2 at $T = 4.2$ K in dark (solid) and under illumination (dashed) at $T = 4.2$ K; (b) Fourier spectra of SdH oscillation for sample 2 in dark (solid) and under illumination (dashed).

Reliable electron densities and mobilities can be derived from the Shubnikov–de Haas oscillations, for which each subband has an oscillation with its own period. The part of the density of states oscillating in magnetic field, Δg, can be expressed as [4]:

$$\frac{\Delta g(\varepsilon_F)}{g_0} = 2\sum_{s=1}^{\infty} \exp\left(-\frac{\pi s}{\mu_q B}\right) \times \cos\left(\frac{2\pi s(E_F - E_i)}{\hbar\omega_c} - s\pi\right) \frac{2\pi^2 s k_B T/\hbar\omega_c}{\sinh(2\pi^2 s k_B T/\hbar\omega_c)}, \quad (1)$$

which leads to the following expressions for the conductivity tensor components in the 2D case (the Landau level width is assumed to be independent of energy and magnetic field):

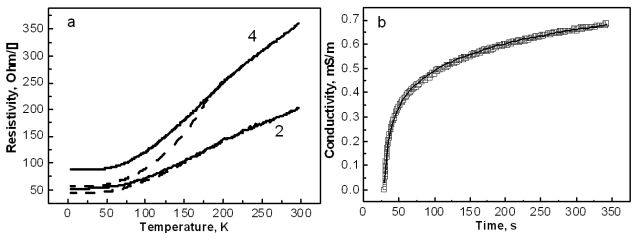

Fig. 3. (a) Temperature dependence of the sheet resistance for sample 2 and 4 in dark (solid line) and after illumination at $T = 4.2$ K (dashed line); (b) relaxation of resistivity of sample 2 at $T = 4.2$ K in dark after illumination. Point are experimental data, solid line is fitting.

$$\sigma_{xx} = \frac{en_s\mu_\mathrm{t}}{1+\mu_\mathrm{t}^2B^2}\left[1+\frac{2\mu_\mathrm{t}B^2}{1+\mu_\mathrm{t}^2B^2}\frac{\Delta g(\varepsilon_\mathrm{F})}{g_0}\right], \quad (2)$$

$$\sigma_{xy} = -\frac{en_s\mu_\mathrm{t}^2B}{1+\mu_\mathrm{t}^2B^2}\left[1-\frac{3\mu_\mathrm{t}^2B^2+1}{\mu_\mathrm{t}^2B^2(1+\mu_\mathrm{t}^2B^2)}\frac{\Delta g(\varepsilon_\mathrm{F})}{g_0}\right], \quad (3)$$

where μ_t is the transport mobility at $B = 0$, g_0 is the density of states at zero magnetic field B, μ_q is the quantum mobility, n_s is the electron density, and e is the absolute value of the electron charge. The oscillation frequency f in the reciprocal magnetic field determines the two-dimensional electron density: $n_s = ef/\pi\hbar$, and the Fermi energy is $E_\mathrm{F} = (\pi\hbar^2/m^*)n_s$.

Scattering through small angles makes a negligible contribution to transport relaxation time. If scattering is large at small angles (in the case of the Coulomb scattering), the transport relaxation time may be an order of magnitude larger than quantum one. Hence the transport mobility is larger than quantum one. Analysis of the oscillation amplitude as a function of magnetic field and temperature yields the transport and quantum mobilities of 2D electrons in each dimensional subband. By varying μ_t and μ_q in each subband, one can fit the theoretical dependence (1–3) of oscillation on magnetic field and FFT to experimental data.

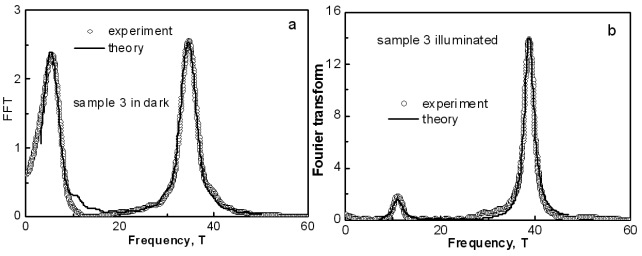

Fig. 4. (a) FFT of SdH oscillation for sample 3 in dark. Point are experimental data, solid line is fitting according to formulae (1)–(3); (b) FFT of SdH oscillation for illuminated sample 3. Point are experimental data, solid line is fitting according to formulae (1)–(3).

As an example the fit to measurements for the sample 3 is shown in Fig. 4a (in dark) and Fig. 4b (illuminated) by the solid line. In this fit we used the optimization technique [4]. The resulting transport and quantum mobilities are listed in Table II. In illuminated samples there is a tendency to higher mobility (both transport and quantum) in both filled subbands. The transport mobility is larger than the quantum mobility. The transport mobility can be derived using the kinetic equation and describing the impurity scattering in the Born approximation. The scattering theory was generalized to the case of several filled subbands in Ref. [6] (see also Refs. [4, 7]). When several dimensional subbands are filled, the transport relaxation times $\tau_{\mathrm{t},i}$ are derived from the linear equation system

$$P_i(E)\tau_{\mathrm{t},i}(E) - \sum_{i\neq i'} P_{ii'}(E)\tau_{\mathrm{t},i}(E) = 1, \quad (4)$$

where the coefficients $P_{ii'}(E)$ are the probabilities for the respective intersubband transitions. The polarization component of the dielectric function was taken from Ref. [8]. The scheme for calculating transport relaxation times in the subbands described in [4]. The quantum lifetime $\tau_{\mathrm{q},i}$ at the Fermi level is obtained by adding all the scattering probabilities with equal weights [9]:

$$\frac{1}{\tau_{\mathrm{q},i}} = \frac{m^*}{\pi\hbar^3}\sum_{i'}\int_0^\pi \mathrm{d}\varphi\left|\tilde{V}_{ii'}(q')\right|^2, \quad \mu_{\mathrm{q},i} = \frac{e}{m^*}\tau_{\mathrm{q},i}. \quad (5)$$

The quantum and transport mobilities in sample 3 calculated by this method are listed in Table III. We also showed in Table III the experimental subband electron concentrations N_SdH which we used for the calculation of the mobility. The dependence of the mobility on the subband number is determined by several competing factors.

On the one hand, the Fermi momentum is lower in the higher subbands, which leads, according to the well-known properties of Coulomb scattering, to a lower mobility.

On the other hand, the width of the electron localization region is larger in the higher subbands, i.e., the average separation between impurities and electrons is larger, which should result in a higher mobility. Our numerical calculations (see Table III) indicate that the electron mobility decreases with the subband number.

TABLE II

Sheet resistivity ρ, quantum μ_q and transport μ_t mobilities at $T = 4.2$ K.

Sample	ρ [Ω/□]	Subband #	μ_q [cm^2/(V s)]	μ_t [cm^2/(V s)]
1	47.36	1	4300	23000
		2	8300	21000
2 dark	52.5	1	2200	28000
		2	4400	25000
2 illuminated	44.4	1	3500	35000
		2	5000	32000
3 dark	59.9	1	3200	35000
		2	3200	30000
3 illuminated	43.6	1	5070	44000
		2	5200	36000
4 dark	88.69	1	2100	22000
4 illuminated	57.3	1	2700	40000

The mobility in the 2nd subband is less because the wave function spread to the delta-layer where charged impurity scattering is high. The calculated transport mobility (see Table II) is much higher than quantum mobility. The calculations and measurements of mobility's are in a good agreement, and the small discrepancies between the calculations and the Shubnikov–de Haas measurements are, most probably, due to errors in the impurity distribution (which is important for the lower subbands) and in the calculated energy levels and wave functions (which affects mostly the mobility in higher subbands).

4. Conclusion

We investigated the electron transport properties and mobility enhancement in the isomorphic QW structures on InP substrate by changing of doping level and the width d of quantum well $In_{0.53}Ga_{0.47}As$. The maximal mobility was observed for QW width $d = 16$ nm. Persistent photoconductivity was observed in all samples due to spatial separation of carriers. Our numerical calculations indicate that the electron mobility decreases with the subband number. The mobility in the 2nd subband is less because the wave function spread to the delta-layer where charged impurity scattering is high. The calculated transport mobility is much higher than quantum mobility. The calculations and measurements of mobilities are in a good agreement.

References

[1] A.S. Brown, U.K. Mishra, J.A. Henige, M.J. Delaney, *J. Vac. Sci. Technol. B* **6**, 678 (1988).

[2] K. Higuchi, H. Uchiyama, T. Shiota, M. Kudo, T. Mishima, *Semicond. Sci. Technol.* **12**, 475 (1997).

[3] M. Malmkvist, S. Wang, J.V. Grahn, *IEEE Trans. Electron Dev.* **55**, 268 (2008).

[4] V.A. Kulbachinskii, R.A. Lunin, V.G. Kytin, A.S. Bugaev, A.S. Senichkin, *JETP* **83**, 841 (1996).

[5] H.J. Queisser, D.E. Theodorou, *Phys. Rev. B* **33**, 4027 (1986).

[6] E.D. Siggia, P.C. Kwok, *Phys. Rev. B* **2**, 1024 (1970).

[7] P.T. Coleridge, *Phys. Rev. B* **44**, 3793 (1991).

[8] K. Inoue, T. Matsuno, *Phys. Rev. B* **47**, 3771 (1993).

[9] R. Fletcher, E. Zaremba, M. D'Iorio, C.T. Foxon, J.J. Harris, *Phys. Rev. B* **41**, 10649 (1990).